

## LETTERS

# A ribosome-associating factor chaperones tail-anchored membrane proteins

Malaiyalam Mariappan<sup>1</sup>, Xingzhe Li<sup>1,2</sup>, Sandra Stefanovic<sup>1</sup>, Ajay Sharma<sup>1</sup>, Agnieszka Mateja<sup>3</sup>, Robert J. Keenan<sup>3</sup> & Ramanujan S. Hegde<sup>1</sup>

Hundreds of proteins are inserted post-translationally into the endoplasmic reticulum (ER) membrane by a single carboxy-terminal transmembrane domain (TMD)<sup>1</sup>. During targeting through the cytosol, the hydrophobic TMD of these tail-anchored (TA) proteins requires constant chaperoning to prevent aggregation or inappropriate interactions. A central component of this targeting system is TRC40, a conserved cytosolic factor that recognizes the TMD of TA proteins and delivers them to the ER for insertion<sup>2–4</sup>. The mechanism that permits TRC40 to find and capture its TA protein cargos effectively in a highly crowded cytosol is unknown. Here we identify a conserved three-protein complex composed of Bat3, TRC35 and Ubl4A that facilitates TA protein capture by TRC40. This Bat3 complex is recruited to ribosomes synthesizing membrane proteins, interacts with the TMDs of newly released TA proteins, and transfers them to TRC40 for targeting. Depletion of the Bat3 complex allows non-TRC40 factors to compete for TA proteins, explaining their mislocalization in the analogous yeast deletion strains<sup>5–7</sup>. Thus, the Bat3 complex acts as a TMD-selective chaperone that effectively channels TA proteins to the TRC40 insertion pathway.

The final step in TA protein targeting to the mammalian ER is mediated by TRC40 (also called Asn1)<sup>2,4</sup>. This factor interacts directly with TA substrates through their TMD, and on targeting to the ER membrane by means of putative receptor(s) it releases the TA protein in an ATPase-dependent manner for insertion into the lipid bilayer. The yeast homologue of TRC40, termed Get3, has an analogous function in conjunction with its ER receptors Get1 and Get2 (ref. 3), and still poorly understood cytosolic factors Get4 and Get5 (refs 5–10). In both cases, TRC40/Get3 must selectively and efficiently capture TA proteins by recognizing a hydrophobic TMD that is prone to aggregation, inappropriate interactions, or sequestration by other chaperones.

To investigate how TRC40 captures its TA protein cargo efficiently, we reconstituted this event *in vitro* and analysed its requirements (Supplementary Fig. 1). Sucrose-gradient-purified ribosome-nascent chains (RNCs) containing a transfer-RNA-tethered TA protein (Sec61 $\beta$ ) were released with puromycin in the presence of cytosolic fractions. Capture of the radiolabelled Sec61 $\beta$  by TRC40 was assayed by crosslinking. As expected, Sec61 $\beta$  released into a complete cytosol was captured by TRC40 in a TMD-dependent and energy-stimulated manner. TRC40 in size-fractionated cytosol was unable to capture Sec61 $\beta$ , which instead crosslinked to an unidentified protein that we provisionally term p38 (Supplementary Fig. 2). TRC40 capture could be restored by adding back one of the missing fractions. Further fractionation confirmed that this 'capture-stimulating' factor is distinct from TRC40 (Supplementary Fig. 3). Thus, efficient substrate capture

by TRC40 in a complex environment requires an additional protein factor whose absence leads to substrate interactions with non-TRC40 proteins (for example, p38) despite the availability of TRC40.

We postulated that the capture-stimulating factor could be an intermediary that delivers substrates to TRC40. Such a factor should recognize TA substrates in a TMD-dependent manner, be found in fractions that contain 'capture-stimulating' activity, and be observed more easily on TRC40 saturation. Crosslinking analyses of Sec61 $\beta$  overproduced in complete cytosol revealed two interacting partners of about 120 kDa and 35 kDa that met these criteria (Supplementary Fig. 4). Our earlier affinity purification of Sec61 $\beta$  from large-scale translation reactions<sup>2</sup> contained an associated product of about 120 kDa (in addition to the major TRC40 band) that we identified by mass spectrometry as Bat3 (also known as Scythe/Bag6) (Supplementary Fig. 5). Bat3 affinity-purified from reticulocyte lysate co-purified with proteins of about 18 kDa and 35 kDa (Fig. 1a), which we identified by mass spectrometry as Ubl4A and C7ORF20; for the latter of these we propose the name TRC35 (Supplementary Fig. 5). Antibodies against Bat3, Ubl4A or TRC35 could co-immunoprecipitate the other two components, and affinity-depletion of any one of these components resulted in substantial depletion of the other two proteins (Supplementary Fig. 6). Thus, Bat3 is part of a stable heterotrimeric complex in the cytosol.

The TMD-dependent interaction of the Bat3 complex with TA proteins was verified by immunoblotting of Sec61 $\beta$  affinity-purified from *in vitro* translation reactions (Fig. 1b). Furthermore, the TMD-dependent 120-kDa and 35-kDa proteins crosslinked to Sec61 $\beta$  (Supplementary Fig. 4) could be specifically immunoprecipitated under denaturing conditions with anti-Bat3 and anti-TRC35 antibodies, respectively, or under non-denaturing conditions by anti-Ubl4A antibodies (Fig. 1c). Analysis of additional TA-protein TMDs by crosslinking showed that both TRC40 and the Bat3 complex interacted with the ER-targeted VAMP2 and Sed5 TMDs, whereas neither interacted with the TMDs from spontaneously inserting cytochrome *b5* (Cb5) or mitochondrially targeted Fis1 or F1L (Fig. 1d). Differences in TMD hydrophobicity (either length or maximal hydrophobicity) among these substrates seemed to be a key determinant, because altering Sec61 $\beta$  TMD hydrophobicity to match that of Cb5, Fis1 or F1L markedly decreased the interaction with both the Bat3 complex and TRC40 (Fig. 1e, f, and Supplementary Fig. 7). Thus, the Bat3 complex interacts directly with the TMDs of several ER-targeted TA proteins with similar substrate specificity to that of TRC40.

We surmised that the Bat3 complex was responsible for the stimulatory activity needed by TRC40 for efficient substrate capture. In cytosolic fractions that had been immunodepleted (by about 95%) of Bat3 (which also depletes Ubl4A and TRC35 without affecting

<sup>1</sup>Cell Biology and Metabolism Program, National Institute of Child Health and Human Development, National Institutes of Health, Bethesda, Maryland 20892, USA. <sup>2</sup>School of Basic Medical Sciences, Peking University, 100191 Beijing, China. <sup>3</sup>Department of Biochemistry and Molecular Biology, 929 East 57th Street, University of Chicago, Chicago, Illinois 60637, USA.

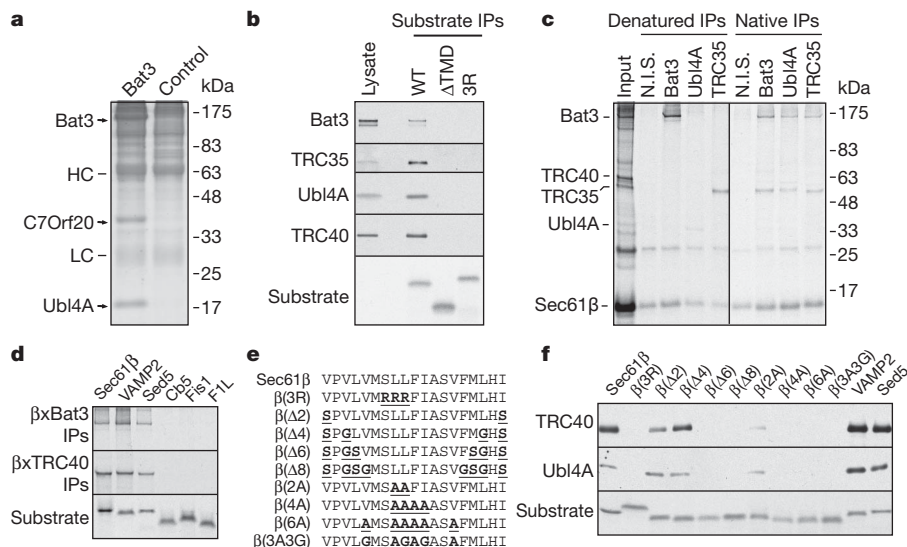


**Figure 1 | Identification of a TMD-interacting protein complex.** **a**, Cytosolic proteins bound and eluted from anti-Bat3 or anti-green fluorescent protein (control) affinity columns are shown. HC and LC are IgG heavy and light chain. **b**, Sec61β (wild type; WT), a deletion construct lacking its TMD (ΔTMD) or the insertion-deficient 3R mutant were translated in reticulocyte lysate, affinity-purified on an anti-Sec61β column and immunoblotted for the indicated products. Total lysate was included for comparison. An autoradiograph of the blot revealed equal recovery of the three translated substrates. IPs, immunoprecipitations. **c**, Crosslinking products of Sec61β (from pooled sucrose-gradient fractions 6–9 in Supplementary Fig. 4) were immunoprecipitated under denaturing or native conditions. Non-immune

serum (N.I.S.) was included as a control. **d**, Versions of Sec61β containing the TMD from the indicated proteins were analysed for interaction with Bat3 and TRC40 by *in vitro* translation, crosslinking and immunoprecipitation. An aliquot of the total translation reaction is shown for each substrate, as well as the immunoprecipitation products of the crosslinking reactions. The Sec61β crosslinked adducts are indicated by 'βx'. **e**, The TMD of Sec61β was mutated as indicated to change its hydrophobicity. **f**, Each construct was analysed for its interactions with the Bat3 complex and TRC40 as in **b**. An aliquot of the total translation product was analysed by autoradiography to reveal the substrates.

TRC40 levels; Fig. 2a and Supplementary Fig. 6), Sec61β capture by TRC40 was diminished, with a concomitant increase in capture by p38 (Fig. 2b); a similar effect was seen with TRC40-immunodepleted extracts, in which p38 was the primary soluble interaction partner. Replenishment of Bat3-depleted extracts to the original level with affinity-purified Bat3 complex (prepared by using an anti-TRC35 antibody (Supplementary Fig. 8)) fully restored TRC40 capture activity (Fig. 2b). The effect of Bat3 depletion on TRC40 substrate capture was not simply a consequence of the RNC-release assay, because translation of full-length TA substrate in Bat3-depleted reticulocyte lysate also showed diminished TRC40 interactions with increased p38 interaction (Supplementary Fig. 9). Thus, maximally efficient capture by TRC40 of TA proteins after their release from the ribosome requires the Bat3 complex. These findings are consistent with recent observations suggesting that depletion of Bat3 can impair the insertion of a TRC40-dependent TA protein<sup>11</sup>.

Although the biochemical functions of Bat3, Ubl4A and TRC35 are poorly understood, the latter two proteins have recognizable homologues in yeast (Mdy2/TMA24/Get5 and Yor164C/Get4, respectively) that have been analysed by recent biochemical, structural and genetic studies<sup>5–7,12,13</sup>. Get4 and Get5 form a stable complex that can interact with Get3, the yeast TRC40 homologue<sup>5,7–10,12,13</sup>. Deletion strains of Get4 and Get5 seem to phenocopy Get1, Get2 or Get3 deletions<sup>5–7</sup>, and all five genes cluster together in synthetic genetic interaction arrays<sup>5,7</sup>. These observations have implicated Get4 and Get5 in TA insertion at a step before Get3, but their functions have been unclear.

Given that the Bat3 complex facilitates TRC40–substrate interactions, we speculated that the Bat3 complex might capture TA substrates at the ribosome and transfer them to TRC40. Such a model would require the Bat3 complex to be at or near the ribosome. Indeed, affinity-purified RNCs containing a TA protein were markedly enriched in the Bat3 complex relative to empty ribosomes (Fig. 3a, b). Quantification showed that the Bat3 complex and signal recognition particle (SRP) occupy about 27% and about 7%, respectively, of TMD-containing RNCs (Fig. 3c). For comparison, SRP occupancy on a genuine SRP substrate isolated by the same method was about 30%

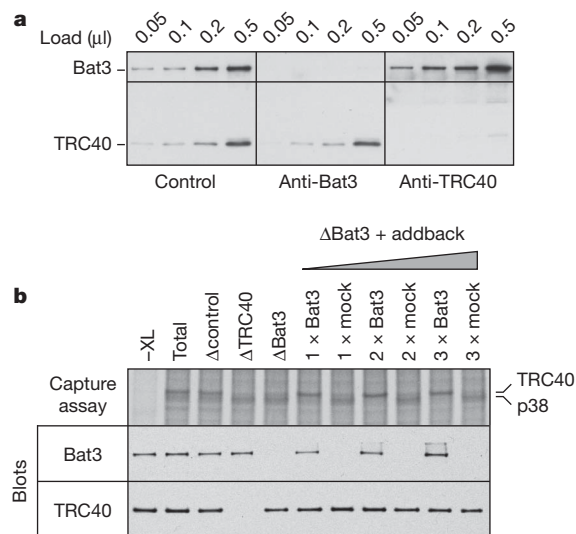


**Figure 2 | The Bat3 complex mediates substrate capture by TRC40.**

**a**, Translation extracts were passed over anti-green fluorescent protein (anti-GFP; control), anti-Bat3 or anti-TRC40 affinity resins and different amounts of each depleted lysate were analysed by immunoblotting. **b**, Substrate capture assay using either total cytosol, or cytosol immunodepleted (Δ) with the indicated affinity resins. In this assay (see Supplementary Fig. 1), radiolabelled Sec61β RNCs were released with puromycin, and capture by TRC40 was assessed by crosslinking. The portion of gel showing the TRC40–Sec61β crosslink is shown. Failure of TRC40 to capture substrate typically results in capture by a 38-kDa protein (p38). The 'addback' lanes are Bat3-depleted cytosol replenished with affinity-purified Bat3 complex (prepared with an anti-TRC35 resin; Supplementary Fig. 8) at three concentrations spanning that present in the original cytosol. The 'mock' addback sample was prepared in parallel but employed an irrelevant affinity resin (anti-GFP) in place of TRC35 affinity resin (Supplementary Fig. 8). A reaction lacking crosslinker (XL) is shown in the left-hand lane. Aliquots of each reaction (before crosslinking) were also analysed by immunoblotting against Bat3 and TRC40 to document their relative amounts in the reactions.

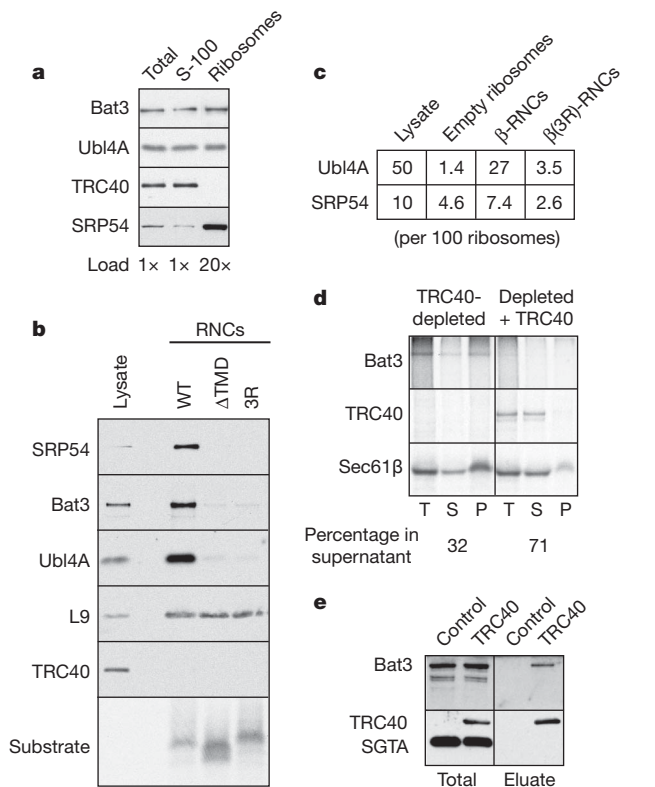


**Figure 3 | The Bat3 complex captures substrates on ribosomes for transfer to TRC40.** **a**, Ribosomes were purified under native conditions from reticulocyte lysate and analysed for TRC40, Bat3, Ubl4A and SRP54 by immunoblotting. About 30–50% of SRP, 2–5% of Bat3 complex, and undetectable (less than 1%) amounts of TRC40 are ribosome-bound. **b**, Affinity-purified and size-purified RNCs (from 60- $\mu$ l translation reactions) of Sec61 $\beta$ , a TMD-lacking version ( $\Delta$ TMD) and the 3R mutant were analysed by immunoblotting for the indicated antigens. For comparison, 0.5  $\mu$ l of translation lysate was analysed. L9 is a ribosomal protein. Autoradiography confirmed equal recovery of each substrate. **c**, The amounts of ribosomes, Ubl4A and SRP54 were quantified in total lysate, purified empty ribosomes and purified RNC preparations. Shown are the amounts of SRP54 and Ubl4A, normalized to 100 ribosomes, averaged from multiple independent purifications ( $n = 3$  for empty ribosomes,  $n = 7$  for Sec61 $\beta$ -RNCs, and  $n = 6$  for  $\beta$ (3R)-RNCs). **d**, Translations of Sec61 $\beta$  in TRC40-depleted lysates lacking or replenished with recombinant zebrafish TRC40 were rapidly diluted, crosslinked and separated by centrifugation into soluble and ribosome fractions. Sec61 $\beta$ , Bat3 crosslinks (immunoprecipitated with anti-Bat3) and TRC40 crosslinks are shown in the total (T), soluble (S) and ribosome (P) fractions. **e**, Cytosolic fractions from HT1080 cells lacking or stably overexpressing haemagglutinin (HA)-tagged human TRC40 were bound to anti-HA resin and selectively eluted with tobacco etch virus (TEV) protease (which cleaves between the HA tag and TRC40). The eluted products, along with starting lysates, were analysed by immunoblotting for Bat3, TRC40 or small glutamine-rich tetratricopeptide repeat-containing protein  $\alpha$  (SGTA; a control protein). Note that endogenous TRC40 is present but not visible at this exposure of the blot. Identical results were obtained when elution of the affinity column was with HA peptide instead of TEV protease (data not shown).

(ref. 14; Supplementary Fig. 10). The Bat3 complex occupies less than 5% of either empty ribosomes or RNCs containing a mutant TMD, illustrating substrate selectivity for the Bat3 complex recruitment. We confirmed that our affinity-purified RNC preparations were associated with tRNA, as judged by their sensitivity to alkaline hydrolysis and selective precipitation with cetyl trimethylammonium bromide (CTAB) (Supplementary Fig. 11). Selective enrichment of the Bat3 complex on TA-protein RNCs was also seen with a magnetic bead ‘pull-up’ strategy that minimizes the non-specific recovery of aggregates (Supplementary Fig. 12). Thus, as suggested for SRP<sup>14</sup>, the Bat3 complex seems to be recruited to ribosomes when a functional TMD is inside the ribosomal exit tunnel.

Analysis of various TMDs for their capacity to recruit the Bat3 complex and SRP to the ribosome from inside the tunnel showed a general correlation with hydrophobicity, with genuine ER-targeted TMDs (from Sec61 $\beta$ , VAMP2 and Sed5) showing the highest recruitment (Supplementary Fig. 10). However, a strict concordance seems unlikely, because a moderately hydrophobic Sec61 $\beta$  mutant (3A3G) that fails to interact with the Bat3 complex post-translationally (Fig. 1f) nonetheless mediated its recruitment from inside the ribosome (Supplementary Fig. 10). The Bat3 complex did not crosslink to ribosome-tethered substrate (Supplementary Fig. 13), but only after release with puromycin or translational termination. This behaviour is opposite to that of SRP, which contacts substrates on the ribosome, but not after release. Thus, ribosomes synthesizing TMD-containing proteins can recruit both SRP and the Bat3 complex at a stage before the emergence of the TMD into the cytosol. Both of these complexes stay on the ribosome during further translation (Supplementary Fig. 10), but after substrate release only the Bat3 complex remains associated in a TMD-dependent manner. Because changes in SRP recruitment do not influence Bat3 recovery on RNCs, the two factors may not compete with each other. However, this remains to be determined, because the binding site for the Bat3 complex is not known.

Selective recruitment of the Bat3 complex to ribosomes before TA protein release suggested that this might be the site of initial substrate capture. We therefore looked for a substrate–Bat3–ribosome intermediate after TRC40 depletion. Sec61 $\beta$  translated in a TRC40-depleted lysate was about 70% ribosome-associated, in which state it could be crosslinked to Bat3 (Fig. 3d). When recombinant TRC40 was included in the depleted translation extract, the proportion of Sec61 $\beta$  in the ribosome fraction was decreased to about 30%, crosslinking to Bat3 was lost, and Sec61 $\beta$  in the soluble fraction was crosslinked to TRC40. Non-ribosomal Sec61 $\beta$ –Bat3 complexes can also transfer substrate to TRC40, because incubation of this fraction with TRC40-containing fractions resulted in a decrease in Bat3 crosslinks and a concomitant increase in TRC40 crosslinks (data not shown). Thus, the Bat3 complex is recruited to the ribosome, where it can interact with TA substrates after their translational termination. This putative Bat3–substrate intermediate, whether on the ribosome or free in solution, is then converted into the productive Sec61 $\beta$ –TRC40 targeting complex. Consistent with this model was our finding that Bat3 and TRC40 can interact, as determined by their co-immunoprecipitation under detergent-free conditions (Fig. 3e).

Recruitment of Bat3 to RNCs is restricted to the period between synthesis of the TMD and release from the ribosome (Fig. 4a), a time window that seems exceedingly brief. To explain this conundrum, we measured the recruitment window by performing a time course of TA protein synthesis combined with selective precipitation of tRNA-associated polypeptides with CTAB. Nascent chains available for recruitment of the Bat3 complex would be nearly full-length but would still contain a covalent tRNA. After confirming that these tRNA-associated full-length species can be selectively recovered (Supplementary Fig. 14), we quantified the amount of this population during a time course of Sec61 $\beta$  synthesis. At 5 min into this time course (about 2 min after full-length Sec61 $\beta$  chains were first detected), 50% of full-length Sec61 $\beta$  was precipitated by CTAB (Fig. 4b). This proportion diminished over time as translational termination ensued and completed Sec61 $\beta$  chains accumulated. Comparison of experimental data with theoretical expectations (Supplementary Fig. 15) yielded an estimated  $t_{1/2}$  for Sec61 $\beta$  termination of about 1 min.

Remarkably, Sec61 $\beta$ - $\Delta$ TMD (lacking the TMD) showed substantially less tRNA-associated polypeptide at each time point (Fig. 4b), corresponding to a termination  $t_{1/2}$  of about 15 s. The last 12 codons (containing an epitope tag) of both constructs are identical, arguing against differences in residues close to the peptidyl transferase centre as the basis for differences in termination rate. The translation elongation rate (about 1.5–1.8 s per residue) and the roughly tenfold slower termination rate (relative to elongation) that we measured for

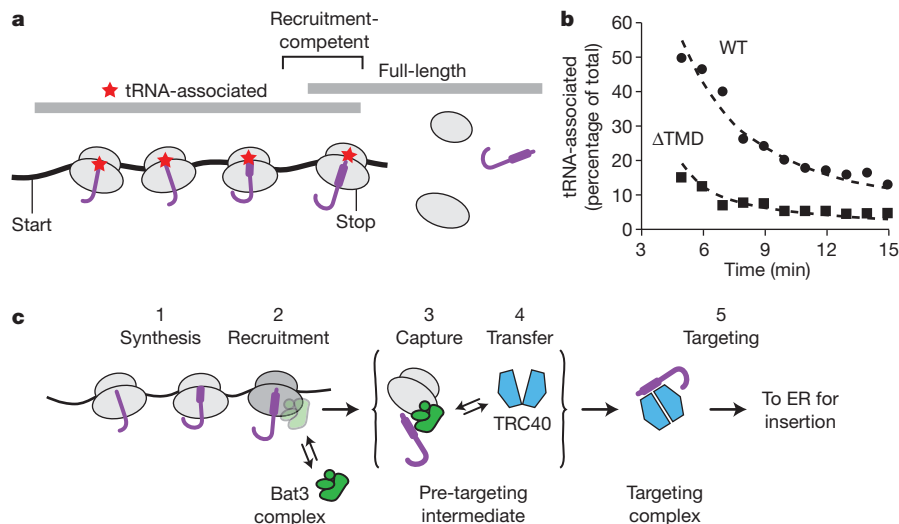


**Figure 4 | Translation termination is delayed for a TA protein.** **a**, Schematic diagram of Sec61 $\beta$  synthesis, illustrating that nascent chains competent for recruitment of the Bat3 complex would be almost full-length and contain a covalently associated tRNA (red star). Such recruitment-competent polypeptides should migrate on gels close to the full-length size but should be precipitated by CTAB, which selectively precipitates tRNA-associated proteins. **b**, Time course of Sec61 $\beta$  and Sec61 $\beta$ ( $\Delta$ TMD) (both tagged at the C terminus with the same 12-residue epitope tag) synthesized at 25 °C in

reticulocyte lysate. At each time point, samples were analysed directly or after CTAB precipitation. The proportion of total full-length polypeptide that was precipitated by CTAB is plotted. The dashed lines indicate theoretical expectations (Supplementary Fig. 15) for a  $t_{1/2}$  of translational termination of 15 and 60 s. **c**, Model for shuttling of TA proteins from the ribosome to TRC40 by means of a pre-targeting intermediate involving recruitment of the Bat3 complex to the ribosome.

our control substrate (Sec61 $\beta$ - $\Delta$ TMD) are consistent with earlier estimates with this same *in vitro* system<sup>15</sup>. However, the unexpectedly long termination rate of Sec61 $\beta$  suggests that the TMD slows this reaction. The magnitude of termination delay seen for Sec61 $\beta$  (about 1 min) is comparable to the elongation ‘arrest’ mediated by SRP measured under similar conditions in this same system<sup>16</sup>. This provides a plausible explanation for how the Bat3 complex could have sufficient time to be recruited to RNCs containing a TMD inside the ribosomal tunnel. The sequence parameters that modulate termination remain to be established, but they are unlikely to depend solely on simple hydrophobicity, given earlier studies showing similar termination delays by relatively hydrophilic sequences<sup>17</sup>.

Our findings explain how the hydrophobic TMDs of TA proteins are safely shielded from inappropriate interactions and aggregation during their delivery to the ER membrane (Fig. 4c). Our working model posits that the TMD is shielded throughout targeting, first by the ribosome, then by the Bat3 complex, and finally by TRC40. The sequential handoffs of substrate between these complexes are likely to be tightly regulated to prevent exposure of the TMD to aqueous solution. Perhaps the Bat3 complex regulates the nucleotide cycle and/or conformation of TRC40 to facilitate its loading with substrate. On the basis of recent crystal structures of Get3 (refs 18–22), efficient substrate loading probably requires a nucleotide-dependent transition from an ‘open’ to a ‘closed’ conformation<sup>18,19</sup> that is perhaps aided by the Bat3 complex. In the absence of this activity, capture by TRC40 would be slower, explaining why it cannot operate efficiently in the presence of competing cytosolic factors but does manage in a purified system (data not shown).

A role for the Bat3 complex in TA protein targeting may therefore not be absolutely essential<sup>23</sup> but would increase fidelity and efficiency. Such a function would seem to be highly conserved, because yeasts have a homologous complex (Get4 and Get5) that shows genetic, physical and functional interactions with Get3 (refs 5–10, 12, 13) and whose absence can lead to aggregation and partial mislocalization of TA proteins<sup>5–7</sup>. Thus, the Bat3 complex seems to represent a conserved TMD-selective chaperone that acts at the ribosome. Where on the ribosome the Bat3 complex binds, how it is recruited when a TMD is inside the ribosomal tunnel, and how its function is coordinated with several other ribosome-associating factors including SRP<sup>24</sup>, nascent

polypeptide-associated complex<sup>25</sup> and ribosome-associated complex<sup>26</sup>, remain important questions for future studies<sup>27</sup>.

## METHODS SUMMARY

**Reagents and standard methods.** Antibodies against Bat3 and Ubl4A were produced in rabbits immunized with recombinant Bat3 fragment (residues 1–250) or full-length Ubl4A, respectively. TRC35 antibodies were against a synthetic peptide (NH<sub>2</sub>-CGSPIELD-COOH) conjugated to keyhole-limpet haemocyanin. *In vitro* transcription, translation in reticulocyte lysate, sucrose-gradient fractionation, chemical crosslinking and immunoprecipitation were performed as described previously<sup>2</sup>. RNCs were generated by transcription and translation of PCR products lacking a stop codon and were sucrose-gradient purified for use in the capture assay. CTAB precipitation of tRNA-associated polypeptides has been described previously<sup>28</sup>.

**RNC release assay.** <sup>35</sup>S-labelled RNCs were incubated with the indicated additions for 15 min at 32 °C. Standard assay conditions were 100 mM potassium acetate, 20 mM HEPES pH 7.4, 7 mM magnesium acetate. The energy-regenerating system consisted of 1 mM ATP, 1 mM GTP, 10 mM creatine phosphate, 40  $\mu$ g ml<sup>-1</sup> creatine kinase. The base cytosolic fraction was prepared from reticulocyte lysate that was bound and eluted from DEAE-Sepharose to remove haemoglobin and concentrated to half the original volume. Immunodepletions from this lysate employed immobilized antibodies. After RNC release, crosslinking was performed with 250  $\mu$ M bismaleimidohexane (a homo-bifunctional cysteine-reactive cross-linker) on ice for 30 min and quenched with 25 mM 2-mercaptoethanol.

**Purification of the Bat3 complex.** Reticulocyte lysate was bound to phenyl-Sepharose, washed in 50 mM HEPES pH 7.4 and eluted with 1% Triton X-100, 50 mM HEPES pH 7.4. The eluate was bound and acid-eluted from anti-Bat3 affinity resin to identify interacting proteins by mass spectrometry. Functional Bat3 complex was isolated from the phenyl-Sepharose fraction with anti-TRC35 resin, eluted with immunizing peptide, and concentrated by binding and elution from S-Sepharose.

**RNC purification.** Affinity purification of size-fractionated RNCs was performed essentially as described previously<sup>24</sup>, but with an antibody against the amino terminus of Sec61 $\beta$  and elution with immunizing peptide. The final RNCs were sedimented to remove any spontaneously released polypeptides.

**Full Methods** and any associated references are available in the online version of the paper at [www.nature.com/nature](http://www.nature.com/nature).

Received 31 January; accepted 18 June 2010.

Published online 1 August 2010.

1. Rabu, C., Schmid, V., Schwappach, B. & High, S. Biogenesis of tail-anchored proteins: the beginning for the end? *J. Cell Sci.* 122, 3605–3612 (2009).

2. Stefanovic, S. & Hegde, R. S. Identification of a targeting factor for posttranslational membrane protein insertion into the ER. *Cell* **128**, 1147–1159 (2007).
3. Schuldiner, M. *et al.* The GET complex mediates insertion of tail-anchored proteins into the ER membrane. *Cell* **134**, 634–645 (2008).
4. Favaloro, V., Spasic, M., Schwappach, B. & Dobberstein, B. Distinct targeting pathways for the membrane insertion of tail-anchored (TA) proteins. *J. Cell Sci.* **121**, 1832–1840 (2008).
5. Jonikas, M. C. *et al.* Comprehensive characterization of genes required for protein folding in the endoplasmic reticulum. *Science* **323**, 1693–1697 (2009).
6. Copic, A. *et al.* Genomewide analysis reveals novel pathways affecting endoplasmic reticulum homeostasis, protein modification and quality control. *Genetics* **182**, 757–769 (2009).
7. Costanzo, M. *et al.* The genetic landscape of a cell. *Science* **327**, 425–431 (2010).
8. Chang, Y. W. *et al.* Crystal structure of Get4–Get5 complex and its interactions with Sgt2, Get3, and Ydj1. *J. Biol. Chem.* **285**, 9962–9970 (2010).
9. Bozkurt, G. *et al.* The structure of Get4 reveals an  $\alpha$ -solenoid fold adapted for multiple interactions in tail-anchored protein biogenesis. *FEBS Lett.* **584**, 1509–1514 (2010).
10. Chartron, J. W., Suloway, C. J. M., Zaslaver, M. & Clemons, W. M. Jr. Structural characterization of the Get4/5 complex and its interaction with Get3. *Proc. Natl Acad. Sci. USA* **107**, 12127–12132 (2010).
11. Leznicki, P., Clancy, A., Schwappach, B. & High, S. Bat3 promotes the membrane integration of tail-anchored proteins. *J. Cell Sci.* **123**, 2170–2178 (2010).
12. Ito, T. *et al.* A comprehensive two-hybrid analysis to explore the yeast protein interactome. *Proc. Natl Acad. Sci. USA* **98**, 4569–4574 (2001).
13. Krogan, N. J. *et al.* Global landscape of protein complexes in the yeast *Saccharomyces cerevisiae*. *Nature* **440**, 637–643 (2006).
14. Berndt, U., Oellerer, S., Zhang, Y., Johnson, A. E. & Rospert, S. A signal-anchor sequence stimulates signal recognition particle binding to ribosomes from inside the exit tunnel. *Proc. Natl Acad. Sci. USA* **106**, 1398–1403 (2009).
15. Lodish, H. F. & Jacobsen, M. Regulation of hemoglobin synthesis: equal rates of translation and termination of  $\alpha$ - and  $\beta$ -globin chains. *J. Biol. Chem.* **247**, 3622–3629 (1972).
16. Wolin, S. L. & Walter, P. Signal recognition particle mediates a transient elongation arrest of preprolactin in reticulocyte lysate. *J. Cell Biol.* **109**, 2617–2622 (1989).
17. Cao, J. & Geballe, A. P. Coding sequence-dependent ribosomal arrest at termination of translation. *Mol. Cell. Biol.* **16**, 603–608 (1996).
18. Mateja, A. *et al.* The structural basis of tail-anchored membrane protein recognition by Get3. *Nature* **461**, 361–366 (2009).
19. Bozkurt, G. *et al.* Structural insights into tail-anchored protein binding and membrane insertion by Get3. *Proc. Natl Acad. Sci. USA* **106**, 21131–21136 (2009).
20. Suloway, C. J., Chartron, J. W., Zaslaver, M. & Clemons, W. M. Jr. Model for eukaryotic tail-anchored protein binding based on the structure of Get3. *Proc. Natl Acad. Sci. USA* **106**, 14849–14854 (2009).
21. Yamagata, A. *et al.* Structural insight into the membrane insertion of tail-anchored proteins by Get3. *Genes Cells* **15**, 29–41 (2010).
22. Hu, J., Li, J., Qian, X., Denic, V. & Sha, B. The crystal structures of yeast Get3 suggest a mechanism for tail-anchored protein membrane insertion. *PLoS ONE* **4**, e8061 (2009).
23. Desmots, F., Russell, H. R., Lee, Y., Boyd, K. & McKinnon, P. J. The Reaper-binding protein Scythe modulates apoptosis and proliferation during mammalian development. *Mol. Cell. Biol.* **25**, 10329–10337 (2005).
24. Halic, M. *et al.* Structure of the signal recognition particle interacting with the elongation-arrested ribosome. *Nature* **427**, 808–814 (2004).
25. Wang, S., Sakai, H. & Wiedmann, M. NAC covers ribosome-associated nascent chains thereby forming a protective environment for regions of nascent chains just emerging from the peptidyl transferase center. *J. Cell Biol.* **130**, 519–528 (1995).
26. Gautschi, M. *et al.* RAC, a stable ribosome-associated complex in yeast formed by the DnaK–DnaJ homologs Ssz1p and zotin. *Proc. Natl Acad. Sci. USA* **98**, 3762–3767 (2001).
27. Kramer, G., Boehringer, D., Ban, N. & Bukau, B. The ribosome as a platform for co-translational processing, folding and targeting of newly synthesized proteins. *Nature Struct. Mol. Biol.* **16**, 589–597 (2009).
28. Hobden, A. N. & Cundliffe, E. The mode of action of alpha sarcin and a novel assay of the puromycin reaction. *Biochem. J.* **170**, 57–61 (1978).

**Supplementary Information** is linked to the online version of the paper at [www.nature.com/nature](http://www.nature.com/nature).

**Acknowledgements** We thank S. Appathurai and M. Downing for technical assistance, Hegde lab members for advice, and J. Weissman and W. Clemons for useful discussions and sharing results before publication. This work was supported by the Intramural Research Program of the National Institutes of Health (R.S.H.) and Edward Mallinckrodt Jr Foundation (R.J.K.).

**Author Contributions** M.M. performed most of the functional analyses of the Bat3 complex, with significant contributions from X.L. during the initial phase of this study. S.S. and R.S.H. developed and characterized the RNC release assay, S.S. initially identified Bat3, and A.S. performed the tRNA-association experiments. A.M. and R.J.K. produced and functionally characterized recombinant proteins, and provided experimental ideas. M.M., X.L., S.S. and R.S.H. analysed data. R.S.H. conceived the project, guided experiments and wrote the paper with input from all authors.

**Author Information** Reprints and permissions information is available at [www.nature.com/reprints](http://www.nature.com/reprints). The authors declare no competing financial interests. Readers are welcome to comment on the online version of this article at [www.nature.com/nature](http://www.nature.com/nature). Correspondence and requests for materials should be addressed to R.S.H. ([hegder@mail.nih.gov](mailto:hegder@mail.nih.gov)).

## METHODS

Most experimental procedures used in this study are minor variations of well-established methods for *in vitro* translocation assays<sup>2</sup>, crosslinking<sup>2</sup>, RNC production and isolation<sup>28</sup>, CTAB precipitation<sup>28</sup> and immunoprecipitation<sup>2</sup>. Specific conditions and variations are provided below and in the figure legends.

**DNA constructs.** The SP64 vector-based constructs encoding wild-type and  $\Delta$ TMD Sec61 $\beta$  appended at the C terminus with an epitope recognized by the 3F4 antibody have been described previously<sup>2</sup>. Mutants of Sec61 $\beta$  (including those in which the entire TMD was replaced with other native TMDs) were generated by either PCR-based site-directed mutagenesis of Sec61 $\beta$ -3F4 (to generate the 3R mutant) or by inserting synthetic oligonucleotides into Sec61 $\beta$ ( $\Delta$ TMD)-3F4 at a unique *Age*I site between the Sec61 $\beta$  cytosolic domain and 3F4 tag. The cyan fluorescent protein (CFP)-tagged Sec61 $\beta$  constructs (Sec61 $\beta$ -CFP and CFP-Sec61 $\beta$ ) have been described previously<sup>2</sup>. Sec61 $\beta$ -TR was generated by inserting synthetic oligonucleotides encoding the TMD of human transferrin receptor (IAVIVFLIGFMIGYLYG) into the *Bgl*I site at codon 50 in the cytosolic domain of Sec61 $\beta$ -3F4. This positions the TMD outside the ribosomal tunnel when the Sec61 $\beta$  TMD is inside the tunnel. The TMD from TR has been experimentally verified to bind SRP as a co-translational substrate<sup>29</sup>. Sec61 $\beta$ -TR\* was generated by inserting the same oligonucleotides in the reverse orientation, thereby coding for an irrelevant hydrophilic sequence (YPKYIPMNPDKKTTITAI). Translations of full-length products was as described previously<sup>2</sup>. To make RNCs, the above constructs were used to PCR amplify the coding region with an SP6 5' primer and a 3' primer lacking a stop codon. For Sec61 $\beta$  and the 3R mutant, the primer anneals at codons 91–96 of Sec61 $\beta$ , after the TMD, but before the epitope tag. For the substrate in which the TMD of Sec61 $\beta$  was replaced with an irrelevant but equal-length hydrophilic spacer sequence, codons encoding the spacer sequence were part of the primer used for PCR amplification. The final product encodes residues 1–66 of Sec61 $\beta$  plus an irrelevant sequence (see Supplementary Fig. 1). These three RNCs are therefore the same length and differ only in the C-terminal region that resides within the ribosomal tunnel. For other RNCs (for example the various mutants and other TMD constructs), the reverse primer annealed in the 3F4 tag or, for the FIL construct, at the end of the TMD. For the Sec61 $\beta$ -CFP RNCs, the reverse primer annealed within the CFP such that the Sec61 $\beta$  TMD was 46 residues away, and therefore outside the ribosomal tunnel.

**Antibodies and proteins.** All custom antibodies were raised in rabbits by Lampire Biological Laboratories. Rabbit polyclonal antibodies against N-terminal and C-terminal peptides within mammalian TRC40 have been described previously<sup>2</sup>. Antibodies against TRC40, Bat3 and Ubl4A were raised in rabbits against full-length human TRC40, residues 1–250 of human Bat3, and full-length human Ubl4A, respectively. These antigens were produced as His-tagged recombinant proteins expressed from the pRSETA vector and purified by Co<sup>2+</sup> affinity chromatography. Antibodies against TRC35 were raised in rabbits against a synthetic peptide (CGSPIELD) conjugated to keyhole-limpet haemocyanin. Recombinant zebrafish TRC40 was expressed as a His-tagged protein and purified as described previously<sup>18</sup>. The Bat3 complex used for functional reconstitution of depleted lysates was purified by a three-step procedure. First, crude ribosome-free reticulocyte lysate was passed over phenyl-Sepharose (the column volume was 0.4 times the volume of lysate). After extensive washing in column buffer (10 mM HEPES pH 7.4, 40 mM potassium acetate, 1 mM magnesium acetate), the bound proteins were eluted with 1% Triton X-100 in column buffer. This eluate was adjusted to 150 mM potassium acetate and 2 mM magnesium acetate, passed over a Protein A resin coupled to anti-TRC35 antibodies (or a control anti-GFP column for the 'mock' addback). After being washed with the same buffer, followed by a low-detergent buffer (25 mM HEPES pH 7.0, 50 mM potassium acetate, 2 mM magnesium acetate, 0.1% Triton X-100), selective elution was performed with 1 mg ml<sup>-1</sup> immunizing peptide in the low-detergent buffer. This eluate was bound to S-Sepharose, washed with detergent-free buffer and step-eluted in 50 mM HEPES pH 7.4, 500 mM potassium acetate, 2 mM magnesium acetate. The concentration relative to starting lysate was quantified by comparative immunoblotting of serial dilutions. Purification of the Bat3 complex in Fig. 1a was from the phenyl-Sepharose elution with anti-Bat3 affinity resin. Control resin contained anti-GFP. Elution was with 0.1 M glycine pH 2.3, 1% Triton X-100.

**Capture assay.** *In vitro* transcription and translation in reticulocyte lysate to generate <sup>35</sup>S-labelled substrate was as described previously<sup>2</sup>. The translation time for RNC preparation was 15 min at 32 °C, after which the samples (volume typically 200  $\mu$ l) were chilled on ice and immediately layered on 2-ml 10–50%

sucrose gradients in physiological salt buffer (PSB; 100 mM potassium acetate, 50 mM HEPES pH 7.4, 2 mM magnesium acetate). Centrifugation was for 1 h at 55,000 r.p.m. at 4 °C in a TLS-55 rotor (Beckman), after which 200- $\mu$ l fractions were removed from the top. The peak ribosomal fractions (6 and 7) were pooled and used as the RNCs. Standard assay conditions were 100 mM potassium acetate, 20 mM HEPES pH 7.4, 7 mM magnesium acetate. The energy-regenerating system consisted of 1 mM ATP, 1 mM GTP, 10 mM creatine phosphate, 40  $\mu$ g ml<sup>-1</sup> creatine kinase. The base cytosolic fraction was prepared from reticulocyte lysate that was bound and eluted from DEAE-Sepharose to remove haemoglobin and concentrated to half the original volume. Release was induced by the addition of puromycin to 1 mM and incubation at 32 °C for 15 min. Crosslinking was performed with 250  $\mu$ M bismaleimidoethane on ice for 30 min and quenched with 25 mM 2-mercaptoethanol.

**RNC affinity purification.** RNCs were affinity-purified with an antibody against the nascent chain, similarly to previous methods<sup>24</sup>. In brief, 300- $\mu$ l translation reactions were subjected to a three-step procedure. Immediately after a 15-min translation reaction, samples were chilled on ice, adjusted to 1  $\mu$ M emetine, and run by gravity over a 1-ml Sephacryl S-300 resin equilibrated in PSB. The void fraction, containing the RNCs but lacking molecules smaller than about 1,500 kDa, was then passed over an anti-Sec61 $\beta$  affinity resin recognizing the extreme N terminus of Sec61 $\beta$  (ref. 30). After being washed with PSB, the bound RNCs were eluted with the immunizing peptide (1.5 mM) in PSB. Finally, the eluate was sedimented at 70,000 r.p.m. in a TL100.2 rotor (Beckman) for 1 h, and the RNC pellet was analysed by immunoblotting. As an alternative strategy in some experiments, the affinity-column step above was replaced by isolation with magnetic beads. Protein A-bound magnetic beads (Dynabeads; Invitrogen) were first pre-bound with the anti-Sec61 $\beta$  antibody, washed and added to the sample (the void fraction from the gel filtration step). After incubation at 4 °C for 1 h, the beads were washed five times with PSB with a magnet to secure the beads on the side of the tube between washes. Elution and subsequent processing was performed as above.

**Miscellaneous biochemistry.** Analysis of crosslinking partners for full-length Sec61 $\beta$  (or its mutant) in individual sucrose gradients and immunoprecipitation to confirm crosslinking adducts was performed as described previously<sup>2</sup>. For denaturing immunoprecipitations, samples after crosslinking were adjusted to 1% SDS, heated, and diluted 1:10 with immunoprecipitation (IP) buffer (1% Triton X-100, 50 mM HEPES pH 7.4 and 100 mM NaCl). Native immunoprecipitations were performed on samples diluted directly into ice-cold IP buffer. SDS-PAGE was conducted on either 8.5% or 12% Tris-tricine gels. The former resulted in separation of p38 crosslinks from TRC40 crosslinks, whereas the latter allowed detection of the roughly 10-kDa substrate. Typically, samples were run on both types of gel in parallel, to resolve the crosslinks and confirm equal sample recovery and loading. The preparation and use of antibody affinity columns was by standard methods. Depletions were performed on columns run by gravity flow. Preliminary experiments were used to determine the minimum amount of resin required to effect at least 90% depletion (as estimated by comparative blotting with serial dilutions). Precipitation with CTAB was conducted as described previously<sup>28</sup>. In brief, samples to be precipitated were adjusted to 2% CTAB, mixed with an equal volume of 0.5 M sodium acetate containing 0.2 mg ml<sup>-1</sup> tRNA from yeast or bovine liver, and incubated at 32 °C for 10 min. The precipitate was collected by centrifugation for 10 min in a micro-centrifuge, washed once in 1% CTAB, 0.25 M sodium acetate at 23 °C, and dissolved in sample buffer for subsequent analysis. CTAB is a denaturing detergent, so translation and other biochemical reactions are instantly stopped on addition to CTAB. Quantification of the Bat3 complex levels in reticulocyte lysate was by semiquantitative immunoblotting of serial dilutions relative to known quantities of purified recombinant Ubl4A. Ribosome levels in lysate were determined by their isolation by sedimentation and measurement of absorbance at 260 nm. Levels of proteins in RNCs were quantified by immunoblotting relative to serial dilutions of lysate (whose abundances of individual proteins was known), purified ribosomes, and/or purified Ubl4A. Multiple independent determinations were made and averaged to generate the values in Fig. 3.

29. High, S., Gorlich, D., Wiedmann, M., Rapoport, T. A. & Dobberstein, B. The identification of proteins in the proximity of signal-anchor sequences during their targeting to and insertion into the membrane of the ER. *J. Cell Biol.* 113, 35–44 (1991).

30. Fons, R. D., Bogert, B. A. & Hegde, R. S. Substrate-specific function of the translocon-associated protein complex during translocation across the ER membrane. *J. Cell Biol.* 160, 529–539 (2003).

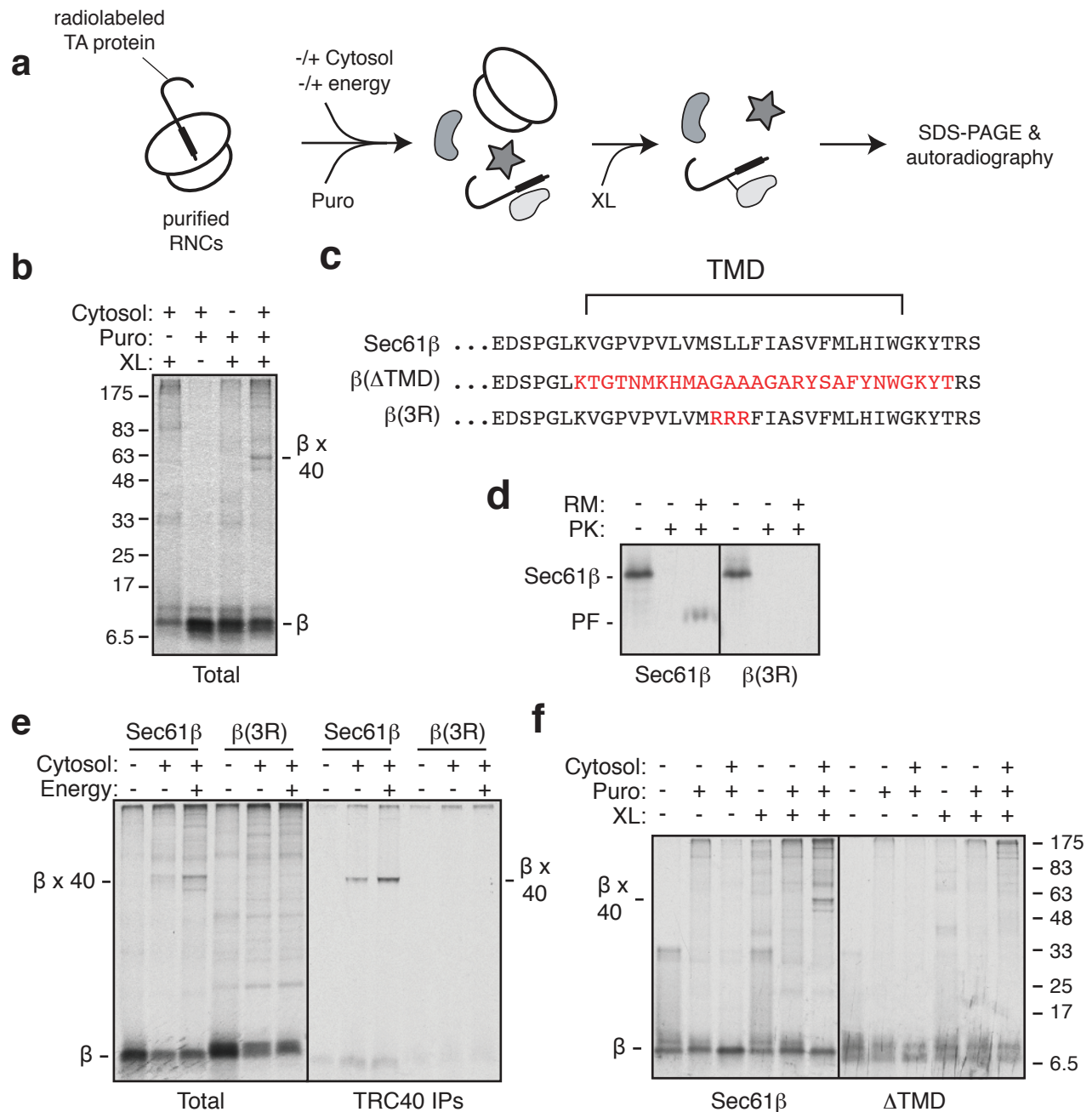


**Fig. S1. In vitro reconstitution and characterization of TA protein capture by TRC40.** (a) Experimental design. Sucrose-gradient purified ribosome-nascent chains (RNCs) of the model TA protein Sec61 $\beta$  are released with puromycin in the presence or absence of cytosolic fractions and an energy regenerating system. The resulting interactions are detected by chemical crosslinking, SDS-PAGE, autoradiography, and/or immunoprecipitation. (b) Purified Sec61 $\beta$  RNCs were treated as indicated and the crosslinks analyzed by SDS-PAGE. The positions of the non-crosslinked Sec61 $\beta$  and the major adduct with TRC40 are indicated. Note that the crosslinked adduct with TRC40 is only observed upon release with puromycin. (c) Sequences of the TMD region of wild type Sec61 $\beta$  and the indicated mutants. Differences from wild type are in red. (d) Validation that the Sec61 $\beta(3R)$  mutant is not competent for insertion. Protease-protection assays for insertion into ER-derived microsomes was performed as before [Stefanovic and Hegde (2007) *Cell* 128:1147-59]. The protected fragment (PF) corresponding to the inserted TMD is indicated. (e) RNCs of wild type Sec61 $\beta$  or Sec61 $\beta(3R)$  were analyzed for capture by TRC40 in the absence or presence of an energy regenerating system. The total products and TRC40 immunoprecipitates (IPs) are shown. Note that the insertion-deficient 3R mutant is not captured by TRC40. (f) Sec61 $\beta$  containing or lacking an intact TMD was analyzed by the RNC release assay as in panel b. Replacement of the TMD with an irrelevant hydrophilic sequence completely abrogates interactions with TRC40. Identical results were obtained when the TMD was simply deleted (data not shown)

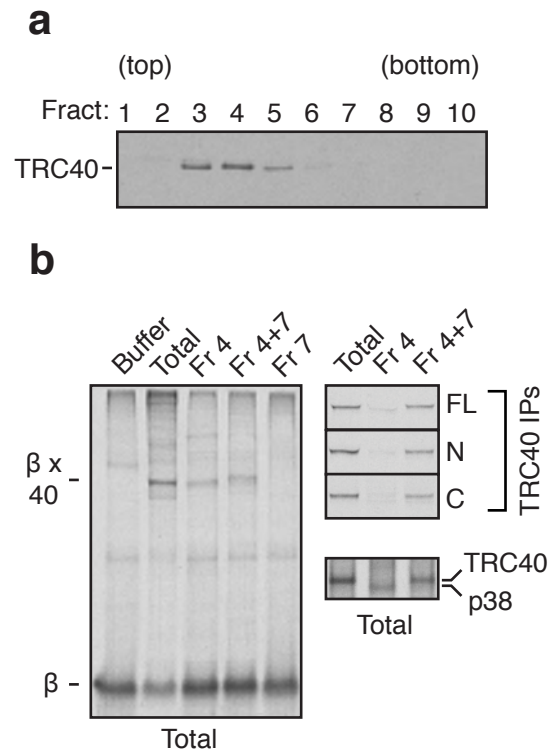


**Fig. S2. An additional factor is needed for substrate capture by TRC40.**(a) Cytosol was fractionated on a 5-25% sucrose gradient and the individual gradient fractions analyzed by immunoblotting for TRC40. The peak of TRC40 is in fraction 4; note that fraction 7 contains little if any TRC40. (b) Substrate capture assay in the indicated sucrose gradient fractions were either analyzed directly (left) or immunoprecipitated with anti-TRC40 antibodies (right). An approximately 40 kD crosslinking partner is seen in three of the lanes. However, the primary crosslink in Fraction 4 cannot be immunoprecipitated by TRC40 antibodies raised against the N-terminus, C-terminus, or full length (FL) protein (upper right panel). On lower percentage gels, this crosslink (p38) can be resolved from crosslinks to TRC40 (lower right panel). This p38 crosslink is lost and TRC40 regained when a mixture of fractions 4 and 7 are used. Since fraction 7 does not itself contain TRC40, this result suggests that fraction 7 contains a factor that facilitates capture of substrate by TRC40. We believe p38 is another cytosolic protein capable of binding hydrophobic sequences since its interaction was TMD-dependent.

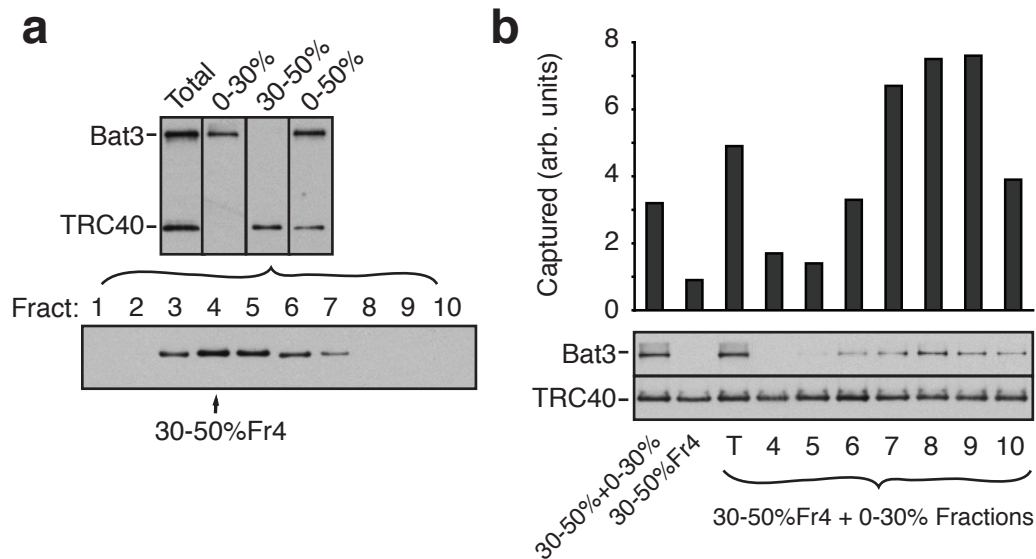


**Fig. S3. Properties of the capture-stimulating activity and co-fractionation with Bat3.** (a) Ammonium sulfate (AS) fractionation and analysis of the fractions by immunoblotting for TRC40 and Bat3. Bat3 is efficiently precipitated by 30% AS, while TRC40 requires 50%. The 30-50% AS cut was further separated on a sucrose gradient, and the peak TRC40-containing fraction (fraction 4) was tested in panel b for its ability to capture Sec61 $\beta$  in the RNC release assay as in Sup. Fig. S1. The 0-30% AS cut was also separated on a sucrose gradient, and the individual fractions tested for their ability to stimulate TRC40 capture of Sec61 $\beta$ . (b) Capture assays of Sec61 $\beta$  RNCs in the indicated fractions. 'T' is the total 0-30% ammonium sulfate fraction, while individual numbers indicate fractions from a sucrose gradient separation of the 0-30% sample. The products of the assay were immunoprecipitated with anti-TRC40 and quantified to assess capture activity. The same samples were also analyzed by immunoblotting for Bat3 and TRC40. Note that maximal capture by TRC40 occurs in fractions containing Bat3. The somewhat lower activity in the crude ammonium sulfate precipitate samples is likely due to inhibition by residual ammonium sulfate. Additional fractionation steps by ion exchange also showed a correlation between Bat3 and capture-stimulating activity (data not shown).

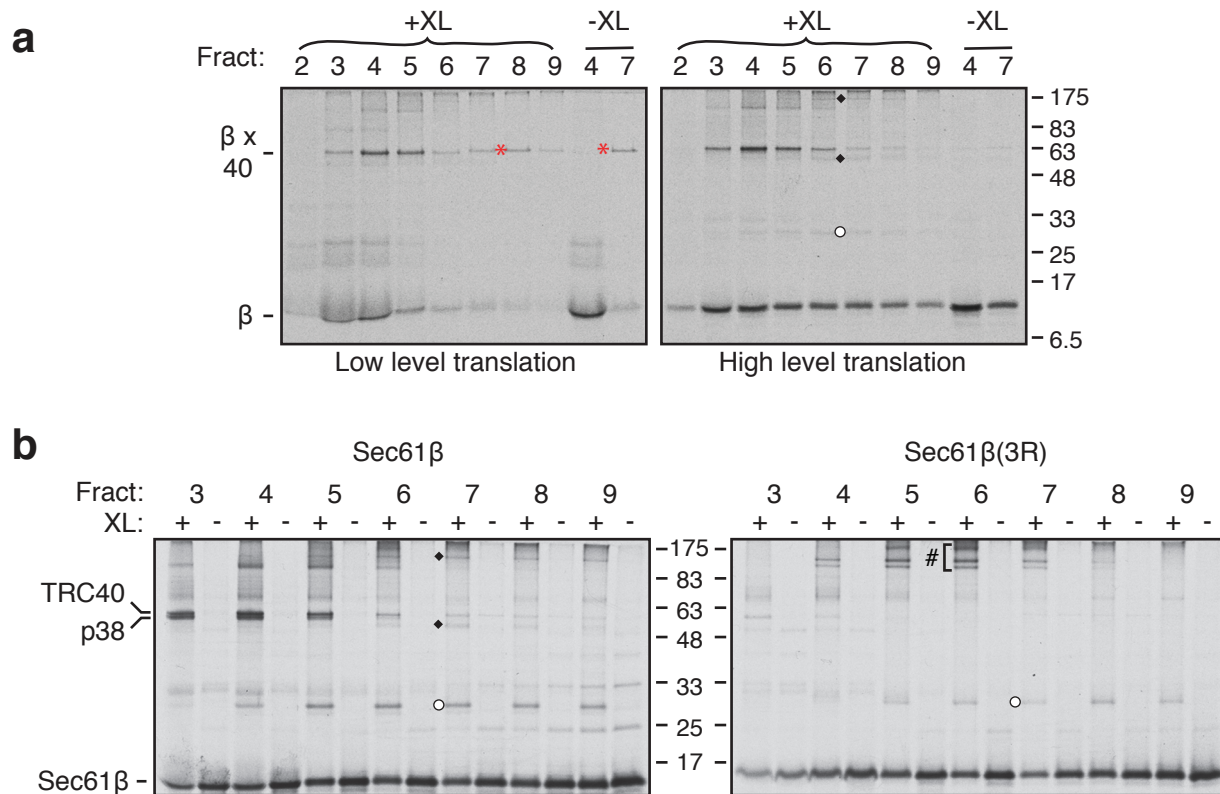


**Fig. S4. Crosslinking reveals candidate proteins for the capture-stimulating factor.** (a) Full length Sec61 $\beta$  was translated in vitro at low or high levels by adjusting the concentration of transcript. Preliminary experiments were used to identify maximal translation conditions (high level), as well as transcript levels needed to produce ~5-fold less product (low level). After translation, the samples were separated on a 5-25% sucrose gradient and each fraction subjected to crosslinking analysis. Aliquots of fractions 4 and 7 in the absence of crosslinker are also shown. Loading of the gel was adjusted such that equal amounts of [<sup>35</sup>S]-labeled Sec61 $\beta$  were analyzed. The major crosslink (to TRC40) in fractions 3-6 is indicated. (b) Sec61 $\beta$  or Sec61 $\beta$ (3R) was translated under 'high level' translation conditions and analyzed for crosslinking to identify interacting partners that are selective to an insertion-competent TMD. The samples without and with crosslinker are shown for fractions 3 to 9. The diamonds and open circles are the same products indicated in panel a. The '#' symbol indicates crosslinks that are unique to the 3R construct. Note that upon saturation of the TRC40 system, crosslinks to p38 can be observed.

Two observations are noteworthy. First, Sec61 $\beta$  migrates more heterogeneously at high levels compared to low levels, with a greater proportion of product seen in the later sucrose gradient fractions (compare the relative amounts of Sec61 $\beta$  in fractions 4 and 7 of the non-crosslinked samples of each translation reaction). Second, this population of Sec61 $\beta$  seen preferentially in the high-level translations is observed to form crosslinks to partners of ~15, 35, and 120 kD. Of these, the 15 kD crosslinking partner (open circle) does not appear to be strictly TMD-dependent (see panel b) and is not Ubl4A, while the ~35 and ~120 kD crosslinking partners (diamonds) proved to be TRC35 and Bat3 in subsequent immunoprecipitation studies.

We estimate by immunoblotting relative to standards that under high-level translation conditions, the amount of Sec61 $\beta$  translated in vitro is ~1 ng/ $\mu$ l, which would exceed by ~2-4-fold the relative molar amount of endogenous TRC40 (i.e., it can be saturated under these conditions).

The band marked by the red asterisk is a reticulocyte protein that becomes non-specifically labeled, and is only observed when samples are over-loaded. Note its presence even in the absence of crosslinker. It can also be seen faintly in the high-level translation samples.

Distortion of the Sec61 $\beta$  band in the low level translation gel is due to co-migrating hemoglobin in the reticulocyte lysate. This distortion is not seen in the high level translation because ~5-fold less translation reaction was loaded.

- a** MEPNSTSTAVEEPDSLEVLVKTLDSQTRTFIVGAQMNVKEFKEHIAASVSIPSEKQRLIYQGRVLQDDKK  
LQEYNVGGKVIHLVERAPPQTHLPSGASSGTGSASATHGGGSPPGTRGPGASVHDRNANSYVMVGTFNLP  
DGSAVDVHINMEQAPIQSEPRVRLVMAQHMIRDIQTLLSRMETLPYLQCRGGPQPQHSQPPPQPPAVTPEP  
VALSSQTSEPVESEAPPREPMEAEEVEERAPAQNPELTPGPAPAGPTPAPETNAPNHPSPAEYVEVLQELQ  
RLESRLQPFLQRYEVLGAAATTDYNNNHEGREEDQRLINLVGESLRLLGNTFVALSDLRCNLACTPPRHL  
HVVRPMSHYTTPMVLQQAAPIQINVGTTVTMTGNGTRPPPTPNAEAPPPGPGQASSVAPSSTNVESSAEG  
APPPGPAPPPATSHPRVIRISHQSVEPVMMHMNIQDSGTQPGGVPSAPTGPLGPPGHGQTLGQQVPGFPT  
APTRVVIARPTPPQARPSHPGGPPVSGTLQGAGLGTNASLAQMVSGLVGQLLMQPVLVAQGTPGMAPPPAP  
ATASASAGTTNTATTAGPAPGGPAQPPPTPQPSMADLQFSQLLGNLLGPAGPGAGGSGVASPTITVAMPGV  
PAFLQGMTDFLQATQTAPPPPPPPPPPPPAEQQTMPPPGSPSGGAGSPGGLGLESLSPEFFTSSVVQGVLS  
SLLGSLGARAGSSESIAAFIQRLSGSSNIFEPGADGALGFFGALLSLLCQNFSMVDVVMLLHGHFQPLQRL  
QPQLRSFFHQHYLGGQEPTPSNIRMATHTLITGLEEYVRESFSLVQVQPGVDIIRTNLEFLQEQFNSIAAH  
VLHCTDSGFGARLLELCNQGLFECLALNLHCLGGQMELAAVINGRIRRMSRGVNPSLVSWLTTMMGLRLQ  
VVLEHMPVGPDAILRYVRRVGDPPQPLPEEPMEVQGAERASPEPQRENASPAPGTTAEEAMSRGPPPAPEG  
GSRDEQDGASAETEPWAAAVPPEWVPIIQQDIQSQRKVKQPPLSDAYLSGMPAKRRKTMQEGEPQLLLSE  
AVSRAAKAAGARPLTSPESLSRDLEAPEVQESYRQQLRSDIQKRLOEDPNYSPQRFPNAQRAFADDP
- b** MAAAAMAEQESARNGGRNRGGVQRVEGKLRASVEKGDYEAHQMYRTLFFRYMSQSKHTEARELMYSGAL  
LFFSHGQONSAADLSMLVLESLEKAEVEVADELLENLAKVFLMDPNSPERVTFVSRALKWSSGGSGKLGH  
PRLHQLLALTLWKEQNYCESRYHFLHSADGEGCANMLVEYSTSRGFRSEVDMFVAQAVLQFLCLKNKSSAS  
VVFTTYTQKHPSIEDGPPFVEPLLNFIWFLLLAVDGGKLTVTFTVLCEYQPSLRRDPMYNEYLDRIGQLFF  
GVPPKQTSSYGLLGNLLTSLMGSSEQEDGEESPSDGSPIELD
- c** MQLTVKALQGRECSLQVPEDELVSTLKQLVSEKLNPVVRQORLLFKGKALADGKRLSDYSIGPNSKLNLVV  
KPLEKVLLEEGEAQLADSPPPQVWLISKVLARHFSAADASRVLEQLQRDYERSLSRLTLDDIERLASRF  
LHPEVTETMEKGFSK

Red = antigen for antibody  
Yellow = Peptide identified by MS  
Underlined = conserved domains

**Supplementary Fig. S5.** Sequences of human Bat3 (a), TRC35 (b), and Ubl4A (c) annotated to indicate the peptides identified by MS/MS (yellow), regions used for antibody production (red), and recognizable domains (underlined). In Bat3, the N-terminal region contains a ubiquitin-like (Ubl) domain, and the C-terminal region contains a putative BAG domain. The N-terminal region of Ubl4A contains a Ubl domain.

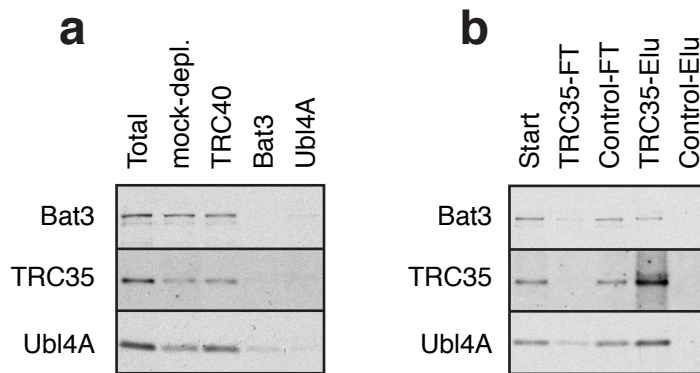
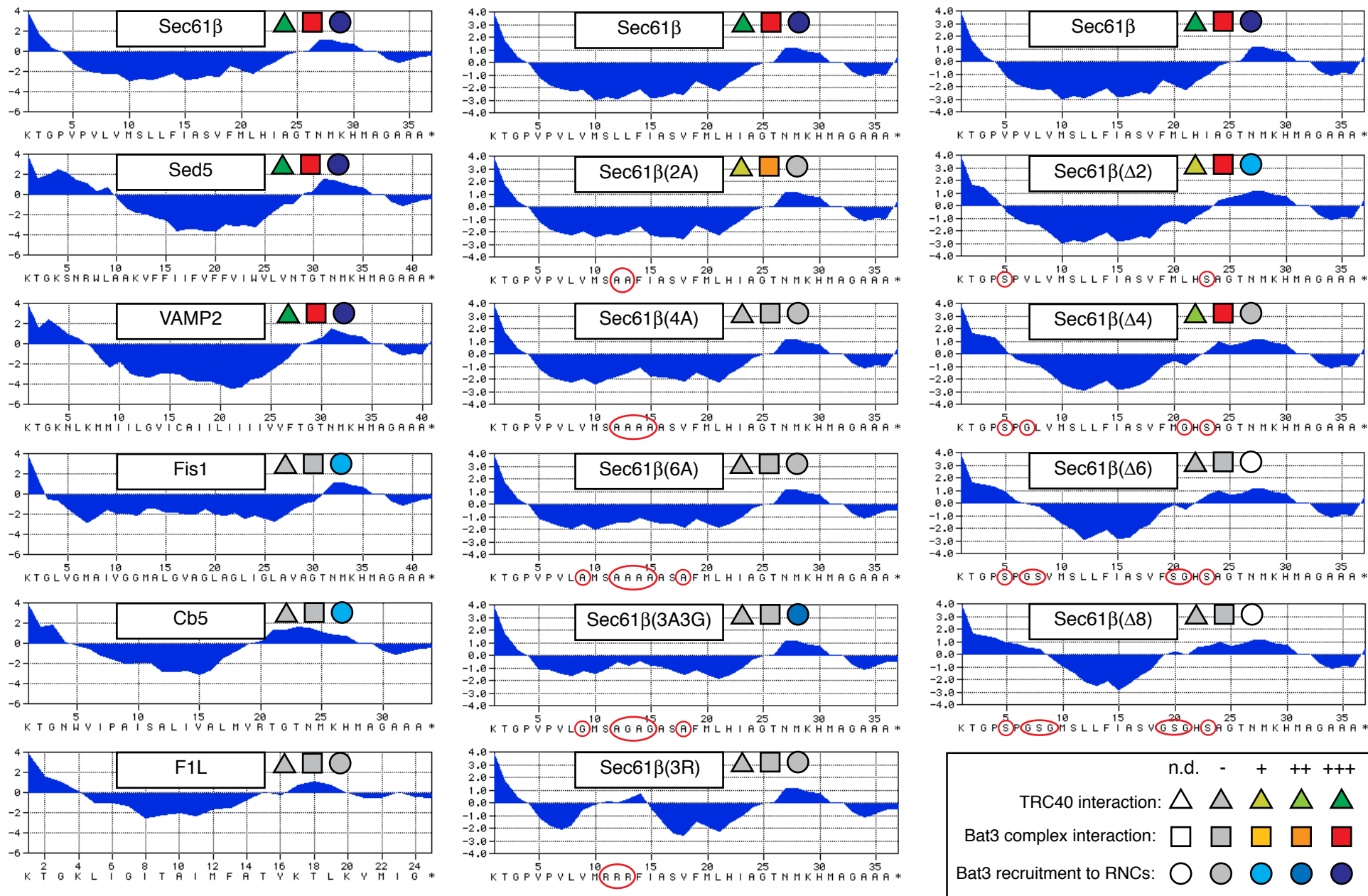
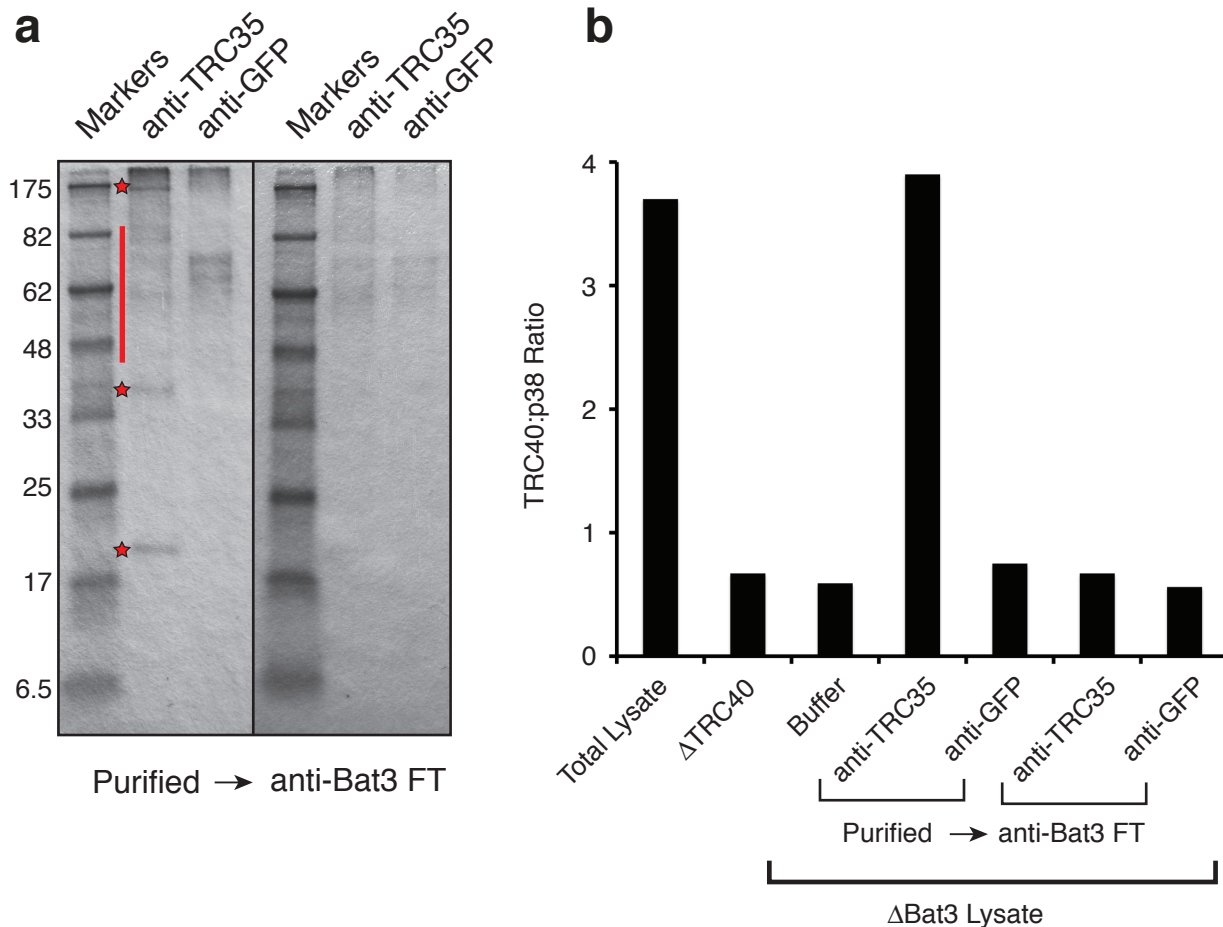


**Fig. S6. Characterization of Bat3 complex interactions.** (a) Depletion of Bat3 or Ubl4A co-depletes the other complex components. A reticulocyte cytosolic fraction (total) was passed over affinity columns containing control antibodies (to GFP; 'mock'), anti-TRC40, anti-Bat3, or anti-Ubl4A. The flow-through fractions from each column were analyzed by immunoblotting. We estimate that depletion of Bat3 results in ~70-80% depletion of Ubl4A and TRC35, with no effect on TRC40 (see Fig. 4A). (b) Co-purification of Bat3 and Ubl4A by TRC35 affinity chromatography. Reticulocyte lysate proteins eluted from a phenyl-sepharose column (start) were passed over either an anti-TRC35 or anti-GFP column (control). After washing, the columns were eluted with the immunizing TRC35 peptide. Aliquots of the flow-through and elution fractions were analyzed by immunoblotting against the Bat3 complex components. TRC40 was not detectable in the purified Bat3 preparations (data not shown).



**Sup. Fig. S7 - Sequences and hydrophobicity of various TA protein constructs.** The last ~40 residues of the indicated TA protein constructs used in this study were analyzed for hydrophobicity using the Kyte-Doolittle scale with window size 7. The left column shows native TMDs, and the other two columns show mutants of the Sec61β TMD (sequence changes indicated by red circles). Wild type Sec61β is shown at the top of each column for comparison. All constructs except F1L contain a C-terminal 3F4 epitope tag (TNMKHMAGAAA). All constructs are in the identical Sec61β context, with the only differences being the TMD. The functional properties of each construct are summarized using the color-coded symbols. A legend to these symbols is at lower left (n.d.= not determined).



**Sup. Fig. S8 - Characterization of immunoaffinity purified Bat3 complex.** (a) Native Bat3 complex purified by affinity chromatography using an anti-TRC35 antibody column (or a parallel anti-GFP control column), followed by concentration and detergent removal by cation exchange, was analyzed by SDS-PAGE and coomassie blue staining (left panel). The red stars indicate the bands corresponding to Bat3, TRC35, and Ubl4A. The red line indicates several apparent contaminants, primarily various IgG species, that leach from the affinity resin. To confirm this conclusion, these purified samples were passed over an anti-Bat3 antibody column, and the flow-thru fraction was analyzed in the right panel. Note that only the three primary bands of the Bat3 complex are selectively and quantitatively removed, while all of the contaminants remain. This indicates two things. First, that only the three proteins indicated are in a stable complex that can be isolated using one antibody (against TRC35) and depleted using another (against Bat3). Second, the other bands observed in the sample are recovered independently of an association with the Bat3 complex. (b) The samples from panel a were assayed for their ability to stimulate substrate capture by TRC40 in a lysate depleted of the Bat3 complex (by an anti-Bat3 resin). As controls, total lysate and TRC40-depleted lysate were analyzed in parallel. Plotted is the ratio of crosslinks to TRC40 versus p38. Note that complementation of the Bat3 depleted lysate with the eluate from the TRC35 affinity resin restored activity, while the control resin eluate had no activity. Importantly, passing the TRC35 eluate over the Bat3 resin completely depleted activity, demonstrating that the remaining contaminants have no activity in facilitating substrate capture by TRC40.

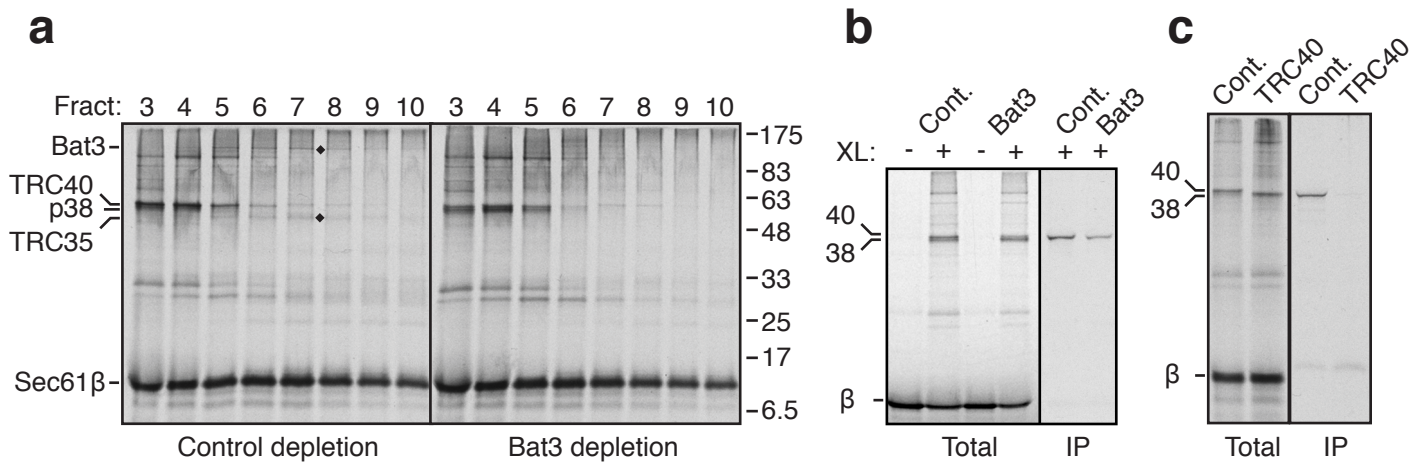
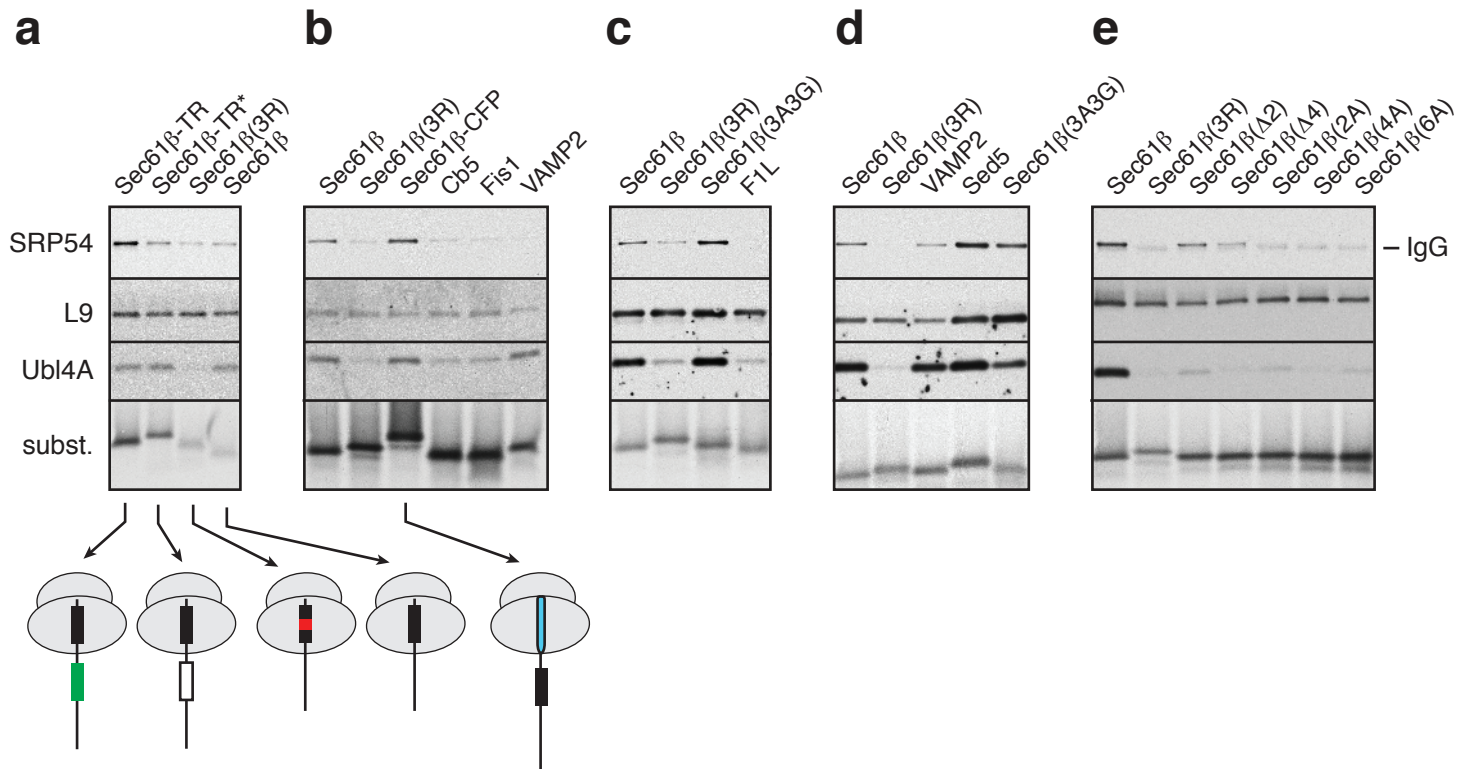


**Fig. S9. Effect of Bat3 depletion on TA protein interactions.** (a) Reticulocyte lysate translation extracts were immunodepleted using an anti-Bat3 or control antibody column and used for translation reactions of full length Sec61 $\beta$ . After translation, the samples were separated by 5-25% sucrose gradients and analyzed by crosslinking of individual fractions. The diamonds indicate crosslinks to Bat3 and TRC35, neither of which are observed in the Bat3-depleted translations. Crosslinks to TRC40 are observed in both translation reactions, but are diminished at the expense of crosslinks to p38 in the Bat3-depleted samples. This is seen more clearly in panel b, where fraction 4 (without and with crosslinker) is analyzed ('total' lanes). Immunoprecipitation with anti-TRC40 ('IP' lanes) and quantification by phosphorimaging verified that capture was reduced by ~60%. Blots of the depleted lysates verified that this reduction in capture was not due to any differences in TRC40 levels, which were identical between the two samples (data not shown). (c) Translation of Sec61 $\beta$  in lysates immunodepleted of TRC40 and analyzed by crosslinking as in panel a shows that TRC40 crosslinks are lost at the expense of p38 crosslinks. Shown are the crosslinking products from fraction 4, and the corresponding TRC40 immunoprecipitates (IP).



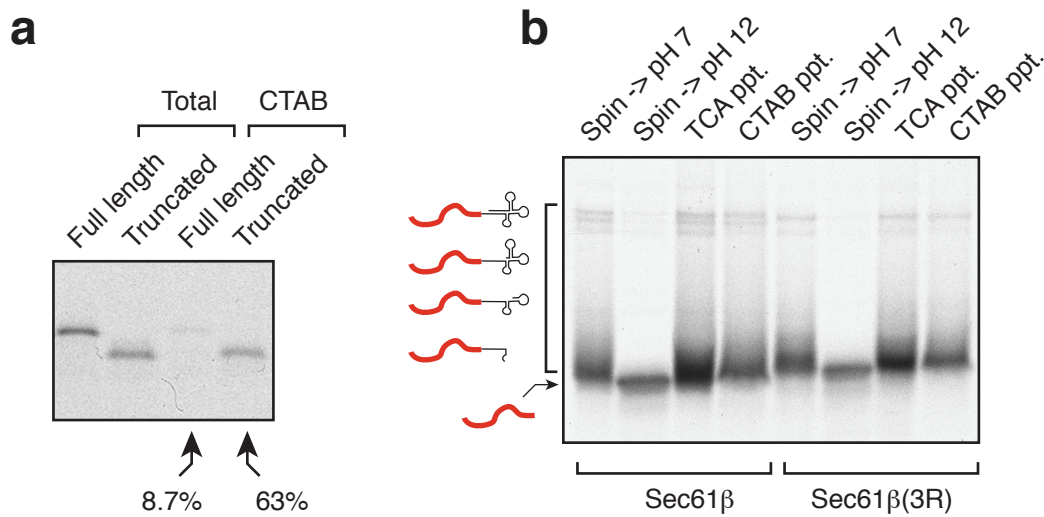
**Sup. Fig. S10. Analysis of SRP and Bat3 complex recruitment to various RNCs.** Panels a through e show different experiments where RNCs of the indicated substrates were immunoaffinity purified using anti-Sec61 $\beta$  and analyzed by immunoblotting against Ubl4A, SRP54, and ribosomal protein L9. The radiolabeled substrate ('subst.') was visualized by autoradiography. The experiment in panel e used magnetic beads containing antibodies that were not crosslinked to the bead, and hence, IgG is seen on the blot close to the SRP54 band.

Shown below some of the samples are schematic diagrams of the RNCs. The black rectangle represents the Sec61 $\beta$  TMD. The green rectangle represents the TMD from transferrin receptor (TR). The white rectangle represents an irrelevant hydrophilic sequence (encoded by the reverse sequence for TR). The black rectangle with red box represents the 3R mutant TMD of Sec61 $\beta$ . The cyan oval is hydrophilic sequence from CFP. The ribosomal tunnel shields ~30-40 residues, and the diagrams indicate this feature by illustrating which portions of the nascent chain are within or outside the ribosome. All other substrates that do not have an accompanying diagram contain the TMD (or mutant TMD) inside the ribosome.

The sequences of the various TMD regions and their accompanying hydrophobicity profiles are shown in Sup. Fig. S7. The sources of the native TMDs that were analyzed are as follows: VAMP2 was from rat; Sed5 was from *S. cerevisiae*; Fis1 was from human; F1L was from a vaccinia virus mitochondrially-targeted TA protein; Cb5 was from rabbit. The mutants either shorten the hydrophobic domain (i.e.,  $\Delta 2$  and  $\Delta 4$ ) or reduce hydrophobicity while maintaining length (i.e., 2A, 4A, 6A, 3A3G).

The following observations are noteworthy. (1) Positioning a TMD outside the ribosome (Sec61 $\beta$ -TR or Sec61 $\beta$ -CFP) increases recruitment of SRP ~3-fold above that seen when a TMD is only inside the ribosome (e.g., Sec61 $\beta$ ). (2) Increased SRP recruitment does not diminish the amount of Bat3 complex. (3) Recruitment of both SRP and Bat3 complex is sensitive to hydrophobicity, and generally follows a similar trend.

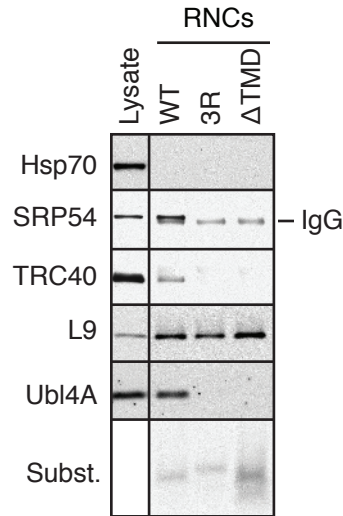
Note that Sec61 $\beta$  and Sec61 $\beta$ (3R) were included in all experiments as controls, and selected other constructs are represented in more than one experiment above. SRP54 is recovered to variable extents in the TMD-disrupted constructs such as the 3R mutant. This may be because of its substrate-independent association with ribosomes. Thus, the extent of washing or time taken during the isolation may influence its recovery in these samples.



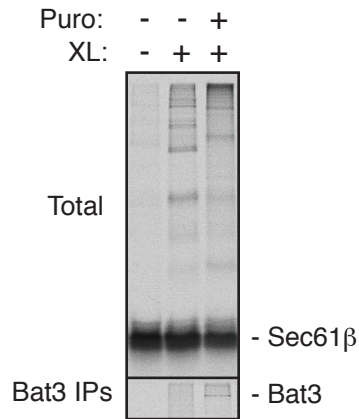
**Sup. Fig. S11. Characterization of affinity purified RNCs for tRNA-association.** (a) Selective precipitation of tRNA-associated, but not terminated, polypeptides using CTAB. Transcript coding for full length Sec61 $\beta$  or a truncated version lacking a stop codon was translated *in vitro* for 15 min at 32°C and analyzed directly ('Total') or subjected to precipitation with CTAB ('CTAB'). Equivalent amounts of sample were analyzed. All samples were treated with pH 12 buffer just before SDS-PAGE to hydrolyze any tRNA. The percent of translation product that is precipitated by CTAB was quantified by phosphorimaging and is shown below the respective lanes. Note that the small amount of CTAB precipitated full length protein was not background, as it was verified in later experiments to be lost upon puromycin treatment, and represents bona fide tRNA-associated product resulting from delayed termination (see Fig. 6). Thus, as characterized in earlier studies, CTAB can be used as a highly selective method to precipitate tRNA-associated polypeptides. (b) Immunoaffinity purified RNCs prepared as in Fig. 5B were divided into four equal aliquots and subjected to the following treatments: (1) Sedimentation to pellet ribosomes, followed by denaturation in pH 7 sample buffer. (2) Sedimentation followed by denaturation in pH 12 sample buffer. (3) Precipitation with trichloroacetic acid (TCA) to recover all products. (4) Precipitation with CTAB to recover tRNA-associated products.

The samples were then analyzed by SDS-PAGE on Tris-tricine gels. Because these gels are run in alkaline conditions (pH 8.5), tRNA is partially hydrolyzed during electrophoresis, resulting in a heterogeneous smear. This is collapsed to a single band upon alkaline treatment (pH 12 samples) or RNase digestion (data not shown). Note that the majority of recovered polypeptides are tRNA associated as judged by either their sensitivity to alkaline treatment or precipitation by CTAB.

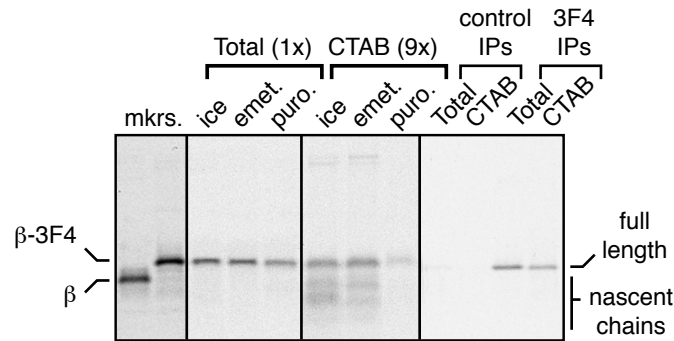
Furthermore, it is worth noting that analysis of RNCs after each step in the purification shows no reduction in the amount of tRNA-associated products recovered (data not shown). In fact, the tRNA-associated products are slightly enriched as the spontaneously hydrolyzed products are removed (especially in the gel filtration step).



**Sup. Fig. S12. Magnetic bead isolation of TA protein RNCs.** An experiment identical to that shown in Fig. 3B was performed using magnetic beads for the immunoaffinity isolation step. After RNCs were produced by *in vitro* translation and stabilized by emetine, they were enriched by gel filtration on Sephacryl S-300 resin. The void fraction (containing the RNCs) was incubated with magnetic protein A beads pre-bound with anti-Sec61 $\beta$  antibodies. After binding, the beads were washed multiple times using a magnet-based 'pull-up' strategy, and eluted by incubation with immunizing Sec61 $\beta$  peptide. The purified RNCs were analyzed by immunoblotting against the indicated antigens. For comparison, 0.5  $\mu$ l of translation extract was analyzed in parallel (and shown from the same exposure as for the RNCs). Because the antibodies used for affinity purification was not immobilized on the magnetic beads, they can be observed just below the SRP54 band. Note that SRP54 and Bat3 complex were recovered in a TMD-dependent manner at high levels relative to their abundance in total lysate. By contrast, Hsp70 is not recovered at all, and TRC40 is found only a low levels, presumably due to its association with Bat3 complex.

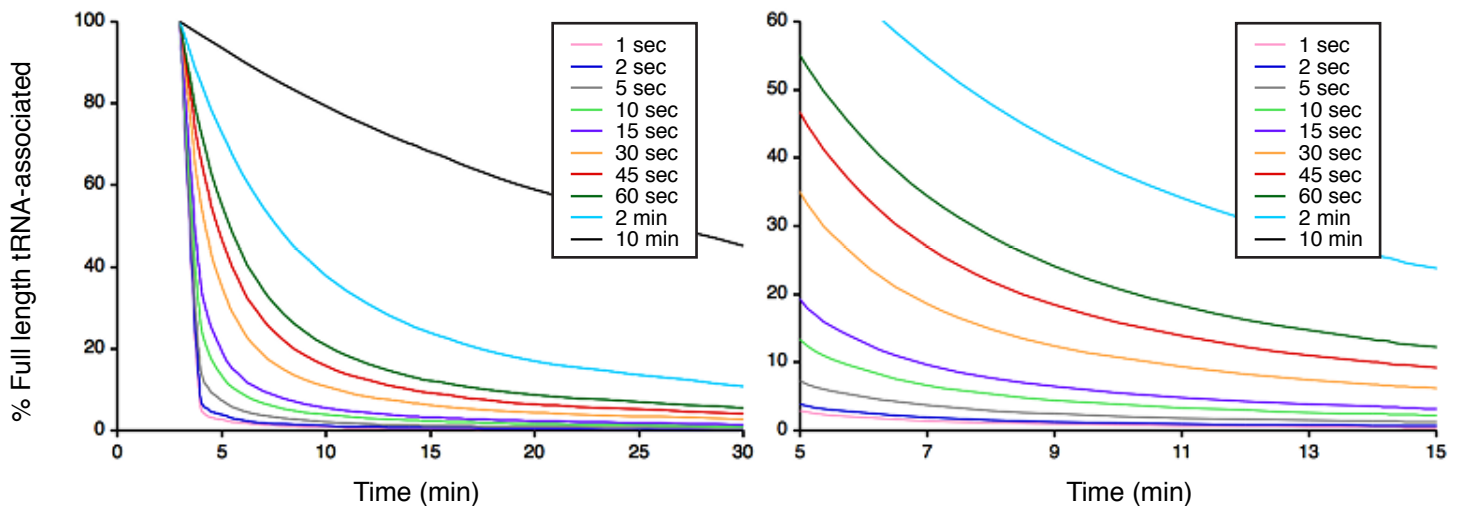


**Sup. Fig. S13. Bat3 interacts with substrates post-translationally.** A cytosolic lysate was fractionated by sucrose gradient sedimentation and a fraction containing Bat3 complex, but not TRC40, was isolated. This Bat3-containing fraction was mixed with Sec61 $\beta$ -RNCs and incubated with or without puromycin as indicated. The samples were then subjected to BMH crosslinking as indicated, and analyzed directly or after immunoprecipitation with anti-Bat3 antibodies. Note that Bat3 crosslinking to substrate was only observed after puromycin release, suggesting that its interaction is primarily post-translational.



**Sup. Fig. S14. Analysis tRNA-associated nascent chains by CTAB precipitation.** Sec61 $\beta$  up to and including the TMD, and Sec61 $\beta$ -3F4 (containing the 12-residue 3F4 epitope tag after the TMD), were synthesized *in vitro* and run as molecular weight markers (first two lanes). Sec61 $\beta$ -3F4 was synthesized for 10 min and either placed on ice, treated with 10  $\mu$ M emetine for 10 min at 32°C, or treated with 1 mM puromycin for 10 min at 32°C. All samples were then analyzed directly ('Total'), after CTAB precipitation (9-fold more was analyzed), or after immunoprecipitation with 3F4 (or control) antibodies.

Nascent chains available for Bat3 complex recruitment would have synthesized the TMD (as judged by near full-length molecular weight), but still contain a covalent tRNA (and hence, be precipitated by CTAB), indicating that termination had not occurred. The above results illustrate the following. First, Sec61 $\beta$  containing a 12-residue 3F4 epitope tag following the TMD could be resolved easily from nascent chains that had not yet synthesized this epitope (but had made the TMD) (lanes 1 and 2). Second, CTAB precipitated products from a brief (10 min) translation reaction of Sec61 $\beta$ -3F4 showed a range of molecular weights enriched in non-full length polypeptides representing partially synthesized nascent chains. Importantly, full length (or nearly so) polypeptides were clearly also precipitated, as verified by immunoprecipitation using 3F4 antibodies. Third, all of these products were markedly reduced if the translation reaction was first treated with puromycin, illustrating that they were functional translation intermediates. Conversely, treatment with emetine, a translation elongation inhibitor, stabilized these products. Thus, by combining CTAB precipitation with high resolution gels, we are able to identify near full length Sec61 $\beta$ -3F4 polypeptides that represent RNCs containing a TMD in the ribosomal tunnel. These nascent chains are precisely those which are able to recruit Bat3 complex, and what was quantified for the time course experiment in Fig. 4.



**Sup. Fig. S15. Modeling of tRNA association for various translation termination rates.** The expected amount of full length tRNA-associated product at various time points was calculated for various termination rates ranging from a  $t_{1/2}$  of 1 sec to 10 min. The following parameters were used: (1) The first completed substrates appear at three minutes (validated by experiment). (2) Translation product accumulation is linear (validated to be true for 15 min in our experiments). (3) Termination follows a simple exponential decay (defined by a  $t_{1/2}$ ). Using these parameters, 100% of full length substrate will be tRNA-associated at 3 min. Before that, all products are tRNA-associated, but none are full length. After 3 min, more substrate continues to be produced, and existing full length tRNA-associated substrate terminates. Plotted on the graph is the proportion of total full length polypeptide (released and tRNA-associated) that is expected to be tRNA associated at any given time (and hence, should be precipitated with CTAB). The two graphs are the same, with the right graph showing only time points from 5 to 15 min, where reliable experimental data can be collected.

Note that although the experimental signal to noise is very low at the earliest time points (less than 5 min), we have indeed observed tRNA-associations approaching 100%, as expected from the predictions. However, the most reliable data is found after 5 min, where the amount of substrate is well above background. Hence, the experimental data in Fig. 4 was from 5 to 15 min, and was compared to the results shown in the right graph above.